Variability of sulfate signal in ice-core records based on five replicate cores

Gautier Elsa[1, 2], Savarino Joël[1, 2], Erbland Joseph[1,2], Lanciki Alyson[1,2], Possenti Philippe[1,2]

[1]Univ. Grenoble Alpes, LGGE, F-38000 Grenoble, France

[2]CNRS, LGGE, F-38000 Grenoble, France

Abstract

Current volcanic reconstructions based on ice core analysis have significantly improved over the past few decades by incorporating multiple core analysis with high temporal resolution from different parts of the Polar Regions. Regional patterns of volcanic deposition are based on composite records, built from cores taken at both poles. However, in many cases only a single record at a given site is used for these reconstructions. This assumes that transport and regional meteorological patterns are the only source of the dispersion of the volcanic-products. Here we evaluate the local scale variability of a sulfate profile in a low accumulation site (Dome C, Antarctica), in order to assess the representativeness of one core for such reconstruction. We evaluate the variability with depth, statistical occurrence, and sulfate flux deposition variability of volcanic eruptions detected on 5 ice cores, drilled 1 meter away from each other. Local scale variability, essentially attributed to snow drift and surface roughness at Dome C, can lead to a non-exhaustive record of volcanic events when a single core is used as the site reference with a bulk probability of 30 % of missing volcanic events and almost 60 % uncertainty on the volcanic flux estimation. Averaging multiple records almost erases the probability of missing volcanic events and can reduce by half the uncertainty pertaining to the deposition flux.

Introduction

When a large and powerful volcanic eruption occurs, the energy of the blast is sufficient to inject megatons of material directly into the upper atmosphere [*Robock*, 2000]. While ashes and pyroclastic materials fall rapidly to the ground because of gravity, gases remain over longer time scales. Among gases, SO_2 is of a particular interest due to its conversion to tiny sulfuric acid aerosols, which can potentially impact the radiative budget of the atmosphere [*Rampino and Self*, 1982; *Timmreck*, 2012]. In the troposphere a combination of turbulence, cloud formation, rainout and downward transport are efficient processes that clean the atmosphere of sulfuric acid, and volcanic sulfuric acid layers rarely survive more than a few weeks, limiting their impact on climate. The story is different when volcanic SO_2 is injected into the stratosphere. There, the dry, cold and stratified atmosphere allows sulfuric acid layers to remain for years, slowly spreading an aerosols blanket around the globe. The tiny aerosols then act as efficient reflectors and absorbers of incoming solar radiations, significantly modifying the energy balance of the atmosphere [*Kiehl and Briegleb*, 1993] and the ocean [*Gleckler et al.*, 2006; *Miller et al.*, 2012; *Ortega et al.*, 2015]. With a lifetime of 2 to 4 years, these aerosols of sulfuric acid ultimately fall into the troposphere where they are removed within weeks.

In Polar Regions, the deposition of the sulfuric acid particles on pristine snow will generate an acidic snow layer, enriched in sulfate. The continuous falling of snow, the absence of melting and the ice thickness make the polar snowpack the best records of the Earth's volcanic eruptions. *Hammer* [1977] was the first to recognize the polar ice propensity to record such volcanic history. Built on the seminal work of Hammer et al., a paleo-volcanism science developed around this discovery with two aims.

The first relies on the idea that the ice record can reveal past volcanic activity and, to a greater extent, its impact on Earth's climate history [*Robock*, 2000; *Timmreck*, 2012]. Indeed, at millennium time scale, volcanoes and the solar activity are the only two recognized natural climate forcings [*Stocker et al.*, 2013]. Based on ice records, many attempts are made to extract the climate forcing induced by a volcanic eruption [*Crowley and Unterman*, 2013 ; *Gao et al*., 2008; *Gao et al*., 2007; *Sigl et al*., 2013; *Sigl et al*., 2014; *Zielinski*, 1995]. However, such an approach is inevitably prone to large uncertainty pertaining to the quality of the ice record and non-linear effects between deposition fluxes and source emissions [*Pfeiffer et al.*, 2006].

The second aim of the paleo-volcanism is to provide an absolute dating scale when clear volcanic events in differently located ice cores can be unambiguously attributed to the same dated event [*Severi et al.*, 2007]. The time synchronization of different proxy records is possible, allowing study of the phasing response of different environmental parameters to climate perturbation [*Ortega et al.*, 2015; *Sigl et al.*, 2015] or estimating the snow deposition over time [*Parrenin et al.*, 2007]. Whatever the intent, paleo-volcanism should rely on robust and statistically relevant ice core records.

Work to establish a volcanic index, undertaken to date, has assumed volcanic event are clearly identified, without any false signal from background variations induced by other sulfur sources (eg marine, anthropogenic, etc.). Seasonal layer counting is used whenever possible, bi-polar comparison of ice sulfate records has become the method of choice to establish an absolute dated volcanic index [*Langway et al.*, 1988]. Both known and unknown events can be used to synchronize different cores. However, only a limited number of peaks, with characteristic shape or intensity, and known to be associated with a dated eruption, can be used to set a reliable time scale [*Parrenin et al.*, 2007]. This restriction is partly fueled by the poor and/or unknown representativeness of most volcanic events found in ice cores. Most of the time, a single core is drilled at a given site and used for cross comparison with other sites. This approach is clearly insufficient for ambiguous events.

At a large scale, sulfate deposition is highly variable in space and mainly associated with atmospheric transport and precipitation patterns. At a local scale (ca. 1m), variability can emerge from post-deposition processes. While sulfate is a non-volatile species supposed to be well preserved in snow, spatial variability is induced by drifted snow, wind erosion leading to surface roughness heterogeneities [*Libois et al.*, 2014]. These effects are amplified in low accumulation sites where most of the deep drilling sites are performed [*EPICA-community-members*, 2004; *Jouzel*, 2013; *Lorius et al.*, 1985]). To the best of our knowledge, one single study has used multiple drillings at a given site to analyze the representativeness of the ice core record [*Wolff et al.*, 2005]. This study took advantage of the two EPICA cores drilled at Dome C, 10 m apart (Antarctica, 75°06'S, 123°21'E, elevation 3220 m, mean annual temperature -54.5°C) [*EPICA-community-members*, 2004] to compare the dielectric profile (DEP) along the 788 m common length of the two cores. For the two replicate cores, statistical analysis showed that up to 50 % variability in the pattern of any given peak was encountered as a consequence of the spatial variability of the snow deposition. The authors concluded that ice-core volcanic indices from single cores at such low-accumulation sites couldn't be reliable and what was required was a network of close-spaced records. However, as mentioned in Wolff's conclusion, this statistical study relied only on two records. Additionally, DEP signals are known to be less sensitive than sulfate signals for volcanic identification, and more accuracy is expected by comparing sulfate profiles. The authors thus encouraged conducting a similar study on multiple ice cores to see if the uncertainty could be reduced.

In the present study we took advantage of the drilling of 5 ice cores at Dome C, initially intended for the analysis of sulfur isotopes of the volcanic sulfate. Putting aside the number of records, our approach is similar in many points to Wolff's work. However, it has the advantage of relying on highly resolved sulfate profiles. In addition, the spatial scale is slightly smaller as the 5 cores were drilled 1-meter apart. The comparison of 5 identically processed cores is a chance to approach the representativeness of a single core reconstruction at a low accumulation site, the most prone to spatial variability. Therefore new constraints on variability of sulfate deposition recorded by spatial heterogeneity in such sites are expected from the present work. Even if recent publications [*Sigl et al.*, 2014], underline the need of using multiple records in low accumulation sites, to overcome the spatial variability issue, such records are not always available. This lack of records adds uncertainty in the volcanic flux reconstruction based on polar depositional pattern. Our study should help to better constrain the error associated with local scale variability, and ultimately, the statistical significance of volcanic reconstructions. The present study discusses the depth shift, occurrence of events and deposition flux variability observed in the 5 cores drilled.

Experimental setup and Methods

Core drilling

The project "VolSol", initiated in 2009, aimed at constraining the estimation of the natural part of radiative forcing, composed of both volcanic and solar contributions using ice core records of sulfate and Beryllium-10. In order to build a robust volcanic index including a discrimination of stratospheric events based on sulfur isotopic ratios [*Baroni et al.*, 2008; *Savarino et al.*, 2003], 5 x 100 m-firn cores (dia. 10 cm) were drilled in 2010/2011 along a 5 m straight line, and spaced approximately 1 m apart. The drilling took place at the French-Italian station Concordia (Dome C, Antarctica, 75°06'S, 123°21'E, elevation 3220 m, mean annual temperature -54.5°C) more precisely between Concordia station and EDC drilling tent (300m west of the EDC drilling tent). At this site, the mean annual snow accumulation rate is about 25 kg m^{-2} y^{-1}, leading to an estimated time-period covered by the cores of 2500 years. Cores were logged and bagged in the field, and temporarily stored in the underground core buffer (- 50 °C) before analysis. The unusual number of ice core drilled at the same place was driven by the amount of sulfate necessary to conduct the isotopic analysis. However, this number of replicate cores drilled 1m apart offers the opportunity to question the representativeness of a volcanic signal extracted from a single core per site.

Sampling, Resolution and IC Analyses

Analyses were directly performed on the field during two consecutive summer campaigns. Thirty meters were analyzed in 2011, the rest was processed the following year. The protocol was identical for each core and the steps followed were:

- Decontamination of the external layer by scalpel scrapping
- Longitudinal cut with a band saw of a 2 cm stick of the most external layer
- Sampling of the ice stick at a 2 cm-resolution (ca. 23 600 samples)
- Thawing the samples in 50 ml centrifuge tubes, and transfer in 15 ml centrifuge tubes positioned in an autosampler
- Automatic analysis with a Metrohm IC 850 in suppressed mode (NaOH at 7 mM, suppressor H_2SO_4 at 50 mM, Dionex AG11 column), in a fast IC configuration (2 min run) with regular calibration (every 60 samples) using certified sulfate reference solution (Fisher brand, 1000 ppm certified).

Due to the fragility of snow cores, the first 4 m were only analyzed on a single core (Figure 1). We will thus not discuss the variability of the Pinatubo and Agung eruptions present in these first 4 meters. Concentration data are deposited in the public domain and made freely available in NOAA National Climatic Data center.

Peaks discrimination method

As with most algorithms used for peak detection, the principle is to detect anomalous sulfate concentration peaks from a background noise (stationary or not), which could potentially indicate a volcanic event. The estimation of the background value should therefore be as accurate as possible. Using core 2 as our reference core, we observed a background average value stationary and close to 85 ppb ± 30 ppb (1σ) at Dome C during the 2,500 years of the record. However, the variability is sufficient enough to induce potential confusion on detection of small peaks. Therefore, a stringent algorithm using PYTHON language (accessible on demand) was developed to isolate each possible peak. The algorithm treats the full ice record by 1-meter section (ca. 45-50 samples). For each meter, a mean concentration (m) and standard deviation (σ) is calculated regardless of the presence or not of peaks in the section. Then, every value above the m + 2 σ is removed from the 1-meter dataset. A new mean and standard deviation is calculated and the same filtration is applied. Iteration runs until no more data above m + 2 σ is found. At that point, m represents the background mean concentration. The process runs for each 1-m section, starting from the surface sample and until the end of the core. Then, each 1-meter dataset is shifted by one sample; the process is reset and the peak detection run again on each new 1-m dataset. Sample shift is applied until the last sample of the first 1-meter section is reached so that no bias is introduced by the sampling scheme. Every concentration data point is thus compared approximately with its 100 neighbor data (50 of each side). Each data point isolated by the algorithm is further tested. To be considered as a point belonging to a potential volcanic peak, the data should be detected in a given core (i.e. for being above the m + 2 σ final threshold) in at least 50 % of the 50 runs. Additionally, the point has to be part of at least three consecutive points passing the same 50 % threshold detection. This algorithm was applied individually on each core, giving 5 different lists of peak. In total, 54, 51, 47, 50 and 47 peaks were detected on core 1, 2, 3, 4 and 5, respectively. A manual detection is then required if one wants to build a more accomplished volcanic record from several profiles, which must be based on shape criteria, and not only statistical criteria. However, in the scope of this paper, no manual sorting was applied, so that the statistical assessment could rely on more objective criteria (the number of occurrences).

Core synchronization and dating

Core 1 was entirely dated with respect to the recently published volcanic ice core database [*Sigl et al.*, 2015] using *Analyseries* 2.0.8 software (http://www.lsce.ipsl.fr/Phocea/Page/index.php?id=3), and covers the time period of -588 to 2010 CE. Figure 2 shows the age-depth profile obtained for this core. A total of 13 major volcanic eruptions well dated were used as time markers to set a time scale (bold date in Table 1). Core 1 was entirely dated through linear interpolation between those tie points. Dated core 1 was then used as a reference to synchronize the remaining 4 cores, using the same tie points and 10 additional peaks (non-bold date in Table 1), presenting characteristic patterns common to each core. In total, 23 points were therefore used to synchronize the cores.

Composite building from the 5 ice cores

Through the routine described above, the five cores are depth-synchronized using the 23 tie points and other potential volcanic events in each core cores are detected independently. Therefore, the number of peaks detected in each core is different (between 47 and 54) and their depth (with the exception of the tie points used) is slightly different to each other cores due to sampling scheme and position of the maximum concentration. After correcting the depth shift between cores, a composite profile was built by summing all the peaks identified in the 5 cores. In this composite, sulfate peaks from different cores are associated to a same event as soon as their respective depth (corresponding to the maximum concentration) are included in a 20cm depth window. This level of tolerance is consistent with the dispersion in width and shape of peaks observed. A number of occurrences is then attributed to each sulfate peak, reflecting the number of time it has been detected in the 5 cores dataset (Figure 4).

Results and Discussions

Depth offset between cores

Depth offsets between cores are the result of the surface roughness at the time of drilling, variability in snow accumulation, heterogeneous compaction during the burying of snow layers and logging uncertainty. This aspect has been discussed previously, over a similar time-scale (Wolff et al. 2005), and over a longer time-scale (Barnes et al. 2006) in Dome C. Surface roughness, attributed to wind speed, temperatures and accumulation rate, is highly variable in time and space. These small features hardly contribute to the depth offset on a larger spatial scale, in which case glacial flow can control the offset between synchronized peaks, as it seems to be the case in South pole site (Bay et al. 2010). However, in Dome C, and at the very local spatial scale we are considering in the present work, roughness is significant regarding to the accumulation rate. It is therefore expected that synchronized peaks should be found at different depths. The offset trend fluctuates with depth, due to a variable wind speed (Barnes et al. 2006). To estimate the variability in the depth shift for identical volcanic events, we used the tie points listed in Table 1. For each peak maximum, we evaluate the depth offset of core 1, 3, 4 and 5, with respect to core 2. To avoid logging uncertainty due to poor snow compaction in the first meters of the cores and surface roughness at the time of the drilling, we used the UE 1809 depth in core 2 (13.30 m) as a depth reference horizon from which all other depth cores were anchored using the same 1809 event. For this reason, only eruptions prior to 1809 were used to evaluate the offset variability, that is 18 eruptions instead of the 23 used for the core synchronization. Figure 5, shows the distribution of depth shift of the cores with respect to core 2. While the first 40 m appear to be stochastic in nature, a feature consistent with the random local accumulation variations associated with snow drift in Dome C site, it is surprising that at greater depth, offset increases (note that the positive or negative trends are purely arbitrary and depends only on the reference used, here core 2). The maximum offset, obtained between core 3 and 5 is about 40 cm. Such accrued offsets with depth were also observed by *Wolff et al.*, [2005] and were attributed to the process of logging despite the stringent guidelines used during EPICA drilling. Similarly, discontinuities in the depth offset, observed by *Barnes et al.,* [2006] were interpreted as resulting from logging errors. As no physical processes can explain a trend in the offsets, we should also admit that the accrued offset is certainly the result of the logging process. In the field, different operators were involved but a common procedure was used for the logging. Two successive cores extracted from the drill were reassembled on a bench to match the non uniform drill cut and then hand sawed meter by meter to get the best precise depth core, as neither the drill depth recorder nor the length of the drilled core section can be used for establishing the depth scale. This methodology involving different operators should have randomized systematic errors but obviously this was not the case. Despite the systematic depth offset observed, synchronization did not pose fundamental issues as the maximum offset in rescaled profiles never exceeds the peak width (ca. 20 cm) thank to the 10 possible comparisons when pair of core are compared. Confusion of events or missing of events are thus very limited in our analysis (see next section).

Variability in events occurrence

The variability in events occurrence in the 5 ice cores has been evaluated through the construction of a composite record (Figure 4) and the counting of events in each core as described in the method. By combining the five ice cores, we listed a total amount of 91 sulfate peaks (Pinatubo and Agung not included), which are not necessarily from volcanic sources. Some peaks can be due to post deposition effects affecting the background deposition, or even contamination. When it comes to defining a robust volcanic index, peak detection issues emerge. Chances to misinterpret a sulfate peak and assign it, by mistake, to a volcanic eruption, as well as chances to miss a volcanic peak, can be discussed through a statistic analysis conducted on our five cores.

We try to evaluate to what extent multiple cores comparison facilitates the identification of volcanic peaks, among all sulfate peaks that can be detected in a core. To do so, we assumed that a peak is of volcanic origin as soon as it is detected at least in two cores. In other words, the probability to have two non-volcanic peaks synchronized in two different cores is nil. It is expected that combining an increasing number of cores will increasingly reveal the real pattern of the volcanic events. All possible combinations from 2 to 5 cores comparison were analyzed, totalizing 26 possibilities for the entire population. The results for each comparison were averaged, giving a statistic on the average number of volcanic peaks identified per number of cores compared. The results of the statistical analysis are presented in Figure 6. As expected, in a composite made of 1 to 5 cores, the number of sulfate peaks identified as volcanic peaks (for being detected at least twice) increases with the number of cores combined in the composite. Thus, while only 30 peaks can be identified as volcanic from a two cores study, a study based on 5 cores can yields 62 such peaks. The 5-cores comparison results in the composite profile given in Figure 4a. The initial composite of 93 peaks is reduced to 64 volcanic peaks (Pinatubo and Agung included) after removing the single peaks (Figure 4b). Each characteristic of the retained peaks is given in Table 2. The main conclusion observing the final composite record is that only 17 of the 64 peaks were detected in all of the 5 cores and 68 % of all peaks were at least present in two cores. At the other side of the spectrum, 2-cores analysis reveals that only 33 % (30 peaks on average) of the peaks are identified as possible eruptions. Two cores comparison presents still a high risk of not extracting the most robust volcanic profile at low accumulation sites, a conclusion similar to *Wolff et al.*, [2005]. Surprisingly, it can also be noticed that this 5-core comparison doesn't results in an asymptotic ratio of identified volcanic peaks, suggesting that 5 cores are not sufficient either to produce a full picture. High accumulation sites should be prone to less uncertainty; however, this conclusion remains an a priori that still requires a confirmation.

Large and small events are not equally concerned by those statistics. Figure 7 shows that the probability of presence is highly dependent on peak flux and the chance to miss a small peak (maximum flux in the window $[f + 2\sigma : f + 5\sigma]$, f being the background average flux) is much higher than the chance to miss a large one (maximum flux above $f + 8\sigma$). However, it is worth noticing that major eruptions can also be missing from the record, as it has already been observed in other studies [*Castellano et al.*, 2005; *Delmas et al.*, 1992]. The most obvious example in our case is the Tambora peak (1815 AD), absent in 2 of our 5 drillings, while presenting an intermediate to strong signal in the others (Figure 8). The reason for the variability in event occurrence has been discussed already by *Castellano et al.*, [2005]. In the present case of close drillings, long-range transport and large-scale meteorological conditions can be disregarded due to the small spatial scale of our study; the snow drift and surface roughness is certainly the main reasons for missing peaks. The fact that two close events as UE 1809 and Tambora are so differently recorded indicates how punctual, in time and space post-depositional effects can affect the recording of eruptions.

Variability in signal strength

To compare peak height variability, detected peaks were corrected by subtracting the background from peak maximum. We considered C_i/C_{mean} variations, C_i being the SO_4^{2-} maximum concentration in core i (1 to 5), and C_{mean} being the mean of those concentration for the event i. For concentration values, positive by definition, the log-normal distribution is more appropriate; geometric means and geometric standard deviations were used, as described by *Wolff et al.*, [2005] (Table 3). In our calculation, the geometric standard deviation based on 2 cores is 1.35; in other words, maximum concentrations are uncertain by a factor 1.35. This factor is slightly lower than the one obtained in *Wolff et al.*, [2005] (1.5). Our cores are drilled closer (one meter from each others, instead of 10 m for *Wolff et al.*), which might slightly reduce the uncertainty. The peaks height variability obtained by averaging 5 cores (1.21), matches *Wolff et al.* forecast. Based on a 50 % uncertainty on 2 cores, *Wolff et al.* predicted a 20 % uncertainty on a 5 cores study (consistent with a reduction of the standard deviation by a factor of $1/\sqrt{n}$, by averaging n values). Comparing the peaks maxima enables us to compare our study with Wolff's study, also based on peaks maxima. However, in our case, comparing maxima induces a bias related to the sampling method: with a two centimeters resolution on average, peak's height is directly impacted by the cutting, which tends to smooth the maxima. Comparing the total sulfate deposited during the event is more appropriate. Proceeding on a similar approach, but reasoning on mass of deposited sulfate rather than maximum concentration, the obtained variability is higher than previously: 41 % uncertainty on volcanic deposited sulfate mass, on a 5-cores study (F_i/F_{mean}, F_i being the mass flux of peak i), and 56 % uncertainty on a 2-cores comparison (F_i/F_1). The difference in the signal dispersion between the two approaches rests on the fact that peak maximum has a tendency to smooth the concentration profile as a consequence of the sampling strategy. This artifact is suppressed when the total mass deposited is considered. In any case, uncertainty seems to be significantly reduced when comparing 5 cores instead of 2.

Conclusion:

This study confirms in many ways previous work on multiple drilling variability [*Wolff et al.*, 2005]. As already discussed, peaks flux uncertainty can be significantly reduced (56 % to 41 %) by averaging 5 ice-cores signals instead of 2. A 5-cores composite profile has been built using the criteria that a peak is considered as volcanic if present at least in two cores. We observed that the number of volcanic peaks listed in a composite profile increases with the number of cores considered. With 2 cores, only 33 % of the peaks present in the composite profile are tagged as volcanoes. This percentage increases to 68 % with 5 cores. However, we did not observe an asymptotic value, even with 5 cores drilled. A record based on a single record in a low accumulation site is therefore very unlikely to be a robust volcanic record. Of course, peaks presenting the largest flux are more likely to be detected in any drilling, but the example of the Tambora shows that surface topography is variable enough to erase even the most significant signal, although rarely. This variability in snow surface is evidenced in the depth offset between two cores drilled less than 5 meters from each other, as peaks can easily be situated 40 cm apart.

In low accumulation sites such as Dome C, where surface roughness can be on the order of the snow accumulation and highly variable, indices based on chemical records should be considered with respect to the time-scale of the proxy studied. Large time-scale trends are faintly sensitive to this effect. On the contrary, a study on episodic events like volcanic eruptions or biomass burning, with a deposition time in the order of magnitude of the surface variability scale should be based on a multiple-drilling analysis. A network of several cores is needed to obtain a representative record, at least in terms of recorded events. However, although lowered by the number of cores, the flux remains highly variable, and still uncertain by a factor of 1.4 with 5 cores. This point is particularly critical in volcanic reconstructions that rely on the deposited flux to estimate the mass of aerosols loaded in the stratosphere, and to a larger extent, the climatic forcing induced. Recent reconstructions largely take into account flux variability associated with regional pattern of deposition, but this study underlines the necessity of not neglecting local scale variability in low accumulation sites. Less variability is expected with higher accumulation rate, but this still has to be demonstrated. Sulfate flux is clearly one of the indicators of the eruption strength, but due to transport, deposition and post-deposition effects, such direct link should not be taken for granted.

With such statistical analysis performed systematically at other sites, we should be able to reveal even the smallest imprinted volcanoes in ice cores, extending the absolute ice core dating, the teleconnection between climate and volcanic events and improving the time-resolution of mass balance calculation of ice sheets.

Acknowledgments

Part of this work would not have been possible without the technical support from the C2FN (French National Center for Coring and Drilling, handled by INSU. Financial supports were provided by LEFE-IMAGO, a scientific program of the Institut National des Sciences de l'Univers (INSU/CNRS), the Agence Nationale de la Recherche (ANR) via contract NT09-431976- VOLSOL and by a grant from Labex OSUG@2020 (Investissements d'avenir – ANR10 LABX56). E. G. deeply thanks the Fulbright commission for providing the PhD Fulbright fellowship. The Institute Polaire Paul-Emile Victor (IPEV) supported the research and polar logistics through the program SUNITEDC No. 1011. We would also like to thank all the field team members present during the VOLSOL campaign and who help us. Data are available at the World Data Center for paleoclimatology (http://www.ncdc.noaa.gov/paleo/wdc-paleo.html).

References

Baroni, M., J. Savarino, J. Cole-Dai, V. K. Rai, and M. H. Thiemens (2008), Anomalous sulfur isotope compositions of volcanic sulfate over the last millennium in Antarctic ice cores, *J Geophys Res*, *113*(D20), D20112, doi: 10.1029/2008jd010185.

Barnes, P. R. F., E. W. Wolff, and R. Mulvaney (2006), A 44 kyr paleoroughness record of the Antarctic surface, J. Geophys. Res., 111, D03102, doi:10.1029/2005JD006349.

Bay, R. C., R. A. Rohde, P. B. Price, and N. E. Bramall (2010), South Pole paleowind from automated synthesis of ice core records, J. Geophys. Res.-Atmos., 115, doi:10.1029/2009jd013741.

Castellano, E., S. Becagli, M. Hansson, M. Hutterli, J. R. Petit, M. R. Rampino, M. Severi, J. P. Steffensen, R. Traversi, and R. Udisti (2005), Holocene volcanic history as recorded in the sulfate stratigraphy of the European Project for Ice Coring in Antarctica Dome C (EDC96) ice core, *J Geophys Res*, *110*(D6), D06114, doi: 10.1029/2004jd005259.

Crowley, T. J., and M. B. Unterman (2013), Technical details concerning development of a 1200 yr proxy index for global volcanism, *Earth Syst. Sci. Data*, *5*(1), 187-197, doi: 10.5194/essd-5-187-2013.

Delmas, R. J., S. Kirchner, J. M. Palais, and J. R. Petit (1992), 1000 years of explosive volcanism recorded at the South-Pole, *Tellus Ser. B-Chem. Phys. Meteorol.*, *44*(4), 335-350.

EPICA-community-members (2004), Eight glacial cycles from an Antarctic ice core, *Nature*, *429*, 623-628, doi: 10.1038/nature02599.

Gao, C., A. Robock, and C. Ammann (2008), Volcanic forcing of climate over the past 1500 years: An improved ice core-based index for climate models, *J Geophys Res*, *113*(D23), D23111, doi: 10.1029/2008jd010239.

Gao, C., L. Oman, A. Robock, and G. L. Stenchikov (2007), Atmospheric volcanic loading derived from bipolar ice cores: Accounting for the spatial distribution of volcanic deposition, *J Geophys Res*, *112*(D9), D09109, doi: 10.1029/2006jd007461.

Gleckler, P. J., K. AchutaRao, J. M. Gregory, B. D. Santer, K. E. Taylor, and T. M. L. Wigley (2006), Krakatoa lives: The effect of volcanic eruptions on ocean heat content and thermal expansion, *Geophys Res Lett*, *33*(17), L17702, doi: 10.1029/2006gl026771.

Hammer, C. U. (1977), Past Volcanism Revealed by Greenland Ice Sheet Impurities, *Nature*, *270*(5637), 482-486.

Jouzel, J. (2013), A brief history of ice core science over the last 50 yr, *Climate of the Past*, *9*(6), 2525-2547, doi: 10.5194/cp-9-2525-2013.

Kiehl, J. T., and B. P. Briegleb (1993), The Relative Roles of Sulfate Aerosols and Greenhouse Gases in Climate Forcing, *Science*, *260*(5106), 311-314, doi: 10.1126/science.260.5106.311.

Langway, C. C., H. B. Clausen, and C. U. Hammer (1988), An inter-hemispheric volcanic time-marker in ice cores from Greenland and Antarctica, *Annals of Glaciology*, *10*, 102-108.

Libois, Q., G. Picard, L. Arnaud, S. Morin, and E. Brun (2014), Modeling the impact of snow drift on the decameter-scale variability of snow properties on the Antarctic Plateau, *Journal of Geophysical*

Research: Atmospheres, *119*(20), 11,662-611,681, doi: 10.1002/2014jd022361.

Lorius, C., J. Jouzel, C. Ritz, L. Merlivat, N. I. Barkov, Y. S. Korotkevich, and V. M. Kotlyakov (1985), A 150,000-year climatic record from Antarctic ice, *Nature*, *316*(6029), 591-596, doi: 10.1038/316591a0.

Miller, G. H., Geirsdóttir, Á., Zhong, Y., Larsen, D. J., Otto-Bliesner, B. L., Holland, M. M., Bailey, D. a., Refsnider, K. a., Lehman, S. J., Southon, J. R., Anderson, C., Björnsson, H. and Thordarson, T. (2012), Abrupt onset of the Little Ice Age triggered by volcanism and sustained by sea-ice/ocean feedbacks, *Geophys. Res. Lett.*, *39*(2), L02708, doi: 10.1029/2011gl050168.

Ortega, P., F. Lehner, D. Swingedouw, V. Masson-Delmotte, C. C. Raible, M. Casado, and P. Yiou (2015), A model-tested North Atlantic Oscillation reconstruction for the past millennium, *Nature*, *523*(7558), 71-74, doi: 10.1038/nature14518.

Parrenin, F., Barnola, J.-M., Beer, J., Blunier, T., Castellano, E., Chappellaz, J., Dreyfus, G., Fischer, H., Fujita, S., Jouzel, J., Kawamura, K., Lemieux-Dudon, B., Loulergue, L., Masson-Delmotte, V., Narcisi, B., Petit, J.-R., Raisbeck, G., Raynaud, D., Ruth, U., Schwander, J., Severi, M., Spahni, R., Steffensen, J. P., Svensson, a., Udisti, R., Waelbroeck, C. and Wolff, E. W. (2007), The EDC3 chronology for the EPICA dome C ice core, *Climate of the Past*, *3*(3), 485-497, doi: 10.5194/cp-3-485-2007.

Pfeiffer, M. A., B. Langmann, and H. F. Graf (2006), Atmospheric transport and deposition of Indonesian volcanic emissions, *Atmos Chem Phys*, *6*, 2525-2537, doi:10.5194/acp-6-2525-2006.

Rampino, M. R., and S. Self (1982), Historic eruptions of Tambora (1815), Krakatau (1883), and Agung (1963), their stratospheric aerosols, and climatic impact, *Quat. Res.*, *18*(2), 127-143, doi: 10.1016/0033-5894(82)90065-5.

Robock, A. (2000), Volcanic eruptions and climate, *Reviews of Geophysics*, *38*(2), 191-219.

Savarino, J., A. Romero, J. Cole-Dai, S. Bekki, and M. H. Thiemens (2003), UV induced mass-independent sulfur isotope fractionation in stratospheric volcanic sulfate, *Geophys Res Lett*, *30*(21), 2131, doi: 10.1029/2003gl018134.

Severi, M., Becagli, S., Castellano, E., Morganti, a., Traversi, R., Udisti, R., Ruth, U., Fischer, H., Huybrechts, P., Wolff, E. W., Parrenin, F., Kaufmann, P., Lambert, F. and Steffensen, J. P. (2007), Synchronisation of the EDML and EDC ice cores for the last 52 kyr by volcanic signature matching, *Clim. Past*, *3*(3), 367-374, doi: 10.5194/cp-3-367-2007.

Sigl, M., Mcconnell, J. R., Layman, L., Maselli, O., Mcgwire, K., Pasteris, D., Dahl-jensen, D., Steffensen, J. P., Vinther, B., Edwards, R., Mulvaney, R. and Kipfstuhl, S. (2013), A new bipolar ice core record of volcanism from WAIS Divide and NEEM and implications for climate forcing of the last 2000 years, *Journal of Geophysical Research: Atmospheres*, *118*(3), 1151-1169, doi: 10.1029/2012jd018603.

Sigl, M., Mcconnell, J. R., Toohey, M., Curran, M., Das, S. B., Edwards, R., Isaksson, E., Kawamura, K., Kipfstuhl, S., Krüger, K., Layman, L., Maselli, O. J., Motizuki, Y., Motoyama, H. and Pasteris, D. R. (2014), Insights from Antarctica on volcanic forcing during the Common Era, *Nature Clim. Change*, *4*(8), 693-697, doi: 10.1038/nclimate2293.

Sigl, M., Winstrup, M., McConnell, J. R., Welten, K. C., Plunkett, G., Ludlow, F., Büntgen, U., Caffee, M., Chellman, N., Dahl-Jensen, D., Fischer, H., Kipfstuhl, S., Kostick, C., Maselli, O. J., Mekhaldi, F., Mulvaney, R., Muscheler, R., Pasteris, D. R., Pilcher, J. R., Salzer, M., Schüpbach, S., Steffensen, J. P., Vinther, B. M. and Woodruff, T. E. (2015), Timing and climate forcing of volcanic eruptions for the past 2,500 years, *Nature*, doi: 10.1038/nature14565.

Stocker, T. F., D. Qin, G.-K. Plattner, M. Tignor, S. K. Allen, J. Boschung, A. Nauels, Y. Xia, B. V., and M. P. M. (2013), IPCC, 2013: The Physical Science Basis, Fifth Assessment Report of the Intergovernmental Panel on Climate Change, Intergovernmental Panel on Climate Change 2013, United Kingdom and New York, NY, USA.

Timmreck, C. (2012), Modeling the climatic effects of large explosive volcanic eruptions, *Wiley Interdiscip. Rev.-Clim. Chang.*, *3*(6), 545-564, doi: 10.1002/wcc.192.

Wolff, E. W., E. Cook, P. R. F. Barnes, and R. Mulvaney (2005), Signal variability in replicate ice cores, *Journal of Glaciology*, *51*(174), 462-468, doi: 10.3189/172756505781829197.

Zielinski, G. A. (1995), Stratospheric loading and optical depth estimates of explosive volcanism over the last 2100 years derived from the Greenland- Ice-Sheet-Project-2 ice core, *J Geophys Res*,

100(D10), 20937-20955.

Table 1 – Tie points used to set the time scale and synchronize the cores. Volcanic events are named "Ev x" if they are not assigned to a well-known eruption. Dating of the events is based on *Sigl et al.*, [2015].

Eruption	core 1	core 2	core 3	core 4	core 5	date of deposition
Surface	0	0	0	0	0	2010
Pinatubo	1.53					**1992**
Krakatoa	8.82	8.92	8.67	8.71	8.63	1884
Cosiguina	11.98	11.83	11.65	11.62	11.46	1835
Tambora	12.85			12.6	12.57	**1816**
UE 1809	13.33	13.3	13.04	13.08	12.98	**1809**
ev 7	15.98	15.93	15.66	15.67	15.52	1762
Serua/UE	19.29	19.22	18.93	18.94	18.78	**1695**
Ev 10	21.87	21.74	21.53	21.48	21.4	1646
kuwae	30.18	30.04	29.92	29.85	29.73	**1459**
ev 16 - A	37.35	37.29	37.17	37.04	36.91	1286
ev 16 - B	37.77	37.77	37.62	37.52	37.4	**1276**
ev 16 - C	38.1	38.04		37.78		1271
Samalas	38.49	38.46	38.28	38.2	38.09	**1259**
ev 17	39.59	39.56	39.46	39.36	39.2	**1230**
ev 18	41.87	41.83	41.7	41.6	41.41	**1172**
ev 22	50.26	50.3	50.2	50.11	49.87	9599
ev 27	60.77	60.72	60.66		60.27	**684**
ev 31	65.72	65.74	65.68	65.6	65.25	**541**
ev 35	76.06	76.13	76	75.94	75.64	235
ev 46	90.42	90.53	90.36	90.41	89.95	**-214**
ev 49	97.15	97.16	97.19	97.22	96.74	**-426**
ev 51	100.16	100.19		100.22	99.7	-529

Table 2 – Sulfate peak (maximum concentration, in $ng.g^{-1}$, and flux of volcanic sulfate deposited, in $kg.km^{-2}$) considered as volcanic eruptions based on the statistical analysis of the 5 cores. Flux is calculated by integrating the peak, using the density profile obtained during the logging process. Volcanic flux values are corrected from background sulfate (calculated separately for each sulfate peak). 0 stands for non-detected events in the cores. Agung (3.77m) and Pinatubo (1.52m) were not included in the statistical analysis because they were analyzed only in core one and thus are marked as not applicable (N/A). The estimation of the average volcanic flux is calculated considering detected peaks only (non detected peaks are not included in this estimation). The relative error on the flux (estimated as 10%) takes into account the IC measurement relative standard deviation (below 4% based on standards runs), the error on firn density (relative error estimated as 2%) and the error on samples time length (10%). The last column displays data obtained from Castellano *et al*. (2005), for identical volcanic peaks. For similar peaks Castellano's flux generally falls into the average flux + 40% uncertainty, sometimes exceeding this value.

Peak depth (m)	date (year)	***core 1***		***core 2***		***core 3***		***core 4***		***core 5***		***average****			***Castellano et al., 2005***	
		$[SO_4^{2-}]$	Volc. flux	$[SO_4^{2-}]$	Volc. flux	$[SO_4^{2-}]$	Volc. flux	$[SO_4^{2-}]$	Volc. flux	$[SO_4^{2-}]$	Volc. flux	$[SO_4^{2-}]$	Volc. flux	*1σ (flux)*	$[SO_4^{2-}]$	Volc. flux
1.52	1992	188	5.0	N/A	N/A	N/A	N/A	N/A	N/A	N/A	N/A	188	5.0	0.5	313	11
3.77	1964	207	5	N/A	N/A	N/A	N/A	N/A	N/A	N/A	N/A	N/A	N/A	N/A	362	8
6.24	1929	0	0.0	164	1.3	0	0.0	132	1.1	0	0.0	148	1.2	0.1		
8.59	1891	0	0.0	0	0.0	0	0.0	134	1.3	117	0.9	126	1.1	0.1	140	3.1
8.92	1885	232	8.1	262	8.8	236	10.5	240	10.2	216	7.7	237	9.1	0.9	289	9.3
11.83	1839	220	7.7	173	5.4	190	4.9	177	5.5	173	4.0	187	5.5	0.6		
12.08	1834	0	0.0	0	0.0	144	2.5	0	0.0	137	1.3	140	1.9	0.2		
12.91	**1816**	455	13.1	0	0.0	0	0.0	188	1.8	307	6.0	317	7.0	0.7	606	39.3
13.3	**1809**	436	16.6	291	10.5	392	12.7	408	16.3	461	13.4	398	13.9	1.4	271	10.2
15.93	**1762**	176	2.7	248	6.7	201	3.4	0	0.0	0	0.0	208	4.2	0.4	174	4.5
19.29	**1695**	287	13.4	0	0.0	168	9.2	194	7.3	0	0.0	217	10.0	1.0	185	8.8
20.3	1674	261	7.8	0	0.0	0	0.0	196	4.3	178	2.3	212	4.8	0.5	142	5.3
20.7	1666	0	0.0	0	0.0	0	0.0	123	1.6	149	2.4	136	2.0	0.2		
21.74	**1646**	257	10.1	249	10.3	259	13.2	282	17.5	257	13.2	261	12.8	1.3		
22.72	1625	181	4.8	146	2.7	141	2.9	0	0.0	0	0.0	156	3.5	0.3	175	8.0
23.77	1600	225	10.6	0	0.0	170	2.5	0	0.0	0	0.0	197	6.5	0.7	194	13.4
25.78	1557	144	2.1	0	0.0	0	0.0	148	2.2	0	0.0	146	2.1	0.2		
30	**1459**	496	33.2	442	31.1	422	31.6	543	37.2	559	36.9	493	34.0	3.4	399	31.7
30.56	1449	0	0.0	143	1.8	131	2.8	0	0.0	0	0.0	137	2.3	0.2		
31.83	1417	0	0.0	0	0.0	0	0.0	155	2.6	148	2.6	151	2.6	0.3		
33.51	1377	0	0.0	0	0.0	140	2.3	0	0.0	162	5.4	151	3.9	0.4		
34.85	1348	273	12.4	288	14.2	209	7.9	303	18.3	269	13.2	268	13.2	1.3	211	10.4
37.29	**1286**	325	18.3	324	16.1	373	17.1	347	14.8	458	30.7	365	19.4	1.9	258	22.4
37.77	**1276**	563	28.9	605	40.4	570	28.8	525	26.3	497	21.6	552	29.2	2.9	304	20.5

38.04	**1271**	205	4.1	180	3.1	0	0.0	235	5.1	0	0.0	206	4.1	0.4		
38.46	**1259**	1086	59.7	1022	63.8	928	61.4	1030	78.5	1428	104.8	1099	73.6	7.4	637	60.4
39.25	1239	0	0.0	0	0.0	132	2.6	147	2.4	151	2.7	143	2.5	0.3		
39.56	**1230**	268	17.8	260	16.8	279	15.6	315	18.7	320	16.7	288	17.1	1.7	337	25.2
41.17	1191	0	0.0	216	4.2	247	12.9	0	0.0	241	7.3	235	8.1	0.8	227	18.0
41.83	**1172**	437	30.9	401	29.4	377	25.2	378	23.3	433	29.4	405	27.6	2.8	311	20.8
44.4	1111	186	5.3	0	0.0	243	5.4	225	9.7	195	6.2	212	6.7	0.7		
44.87	1099	174	2.5	0	0.0	0	0.0	153	2.4	0	0.0	163	2.5	0.2		
45.81	1075	129	1.6	144	2.3	0	0.0	0	0.0	0	0.0	137	2.0	0.2		
47.15	1041	187	3.6	193	3.6	217	4.4	0	0.0	203	6.2	200	4.5	0.4		
47.5	1031	192	7.0	163	5.0	166	3.1	0	0.0	198	4.5	180	4.9	0.5		
48	1018	0	0.0	155	3.2	168	2.8	0	0.0	0	0.0	161	3.0	0.3		
49.63	976	132	2.0	0	0.0	139	2.5	0	0.0	0	0.0	135	2.2	0.2		
50.3	**959**	209	8.2	256	15.6	236	12.6	220	11.9	227	12.1	230	12.1	1.2		
52.49	902	254	3.9	0	0.0	215	4.8	184	5.9	233	7.7	222	5.6	0.6		
54.35	852	0	0.0	0	0.0	0	0.0	155	2.3	249	5.2	202	3.7	0.4		
55.65	819	184	8.8	193	7.3	191	6.7	181	7.1	249	5.2	200	7.0	0.7		
58.26	749	155	3.2	202	3.4	0	0.0	201	6.6	0	0.0	186	4.4	0.4		
60.72	**684**	287	12.9	216	14.0	243	7.8	0	0.0	230	4.9	244	9.9	1.0		
64.49	577	528	36.0	0	0.0	430	25.8	367	21.4	393	23.3	430	26.6	2.7		
65.74	**541**	287	19.1	274	12.7	283	20.5	306	21.5	304	16.3	291	18.0	1.8		
68.41	465	132	2.9	0	0.0	182	4.4	0	0.0	0	0.0	157	3.7	0.4		
69.41	436	194	10.7	168	3.8	0	0.0	207	11.1	233	9.1	201	8.7	0.9		
72.38	352	0	0.0	172	4.7	203	5.3	0	0.0	188	5.8	188	5.3	0.5		
73.13	331	0	0.0	169	4.1	152	2.8	0	0.0	0	0.0	160	3.5	0.3		
73.95	304	0	0.0	0	0.0	171	3.7	190	5.7	0	0.0	180	4.7	0.5		
76.13	**235**	205	12.1	258	20.0	237	21.7	287	23.8	262	13.0	250	18.1	1.8		
77.17	206	179	5.4	206	15.4	211	12.5	219	13.2	272	13.5	217	12.0	1.2		
78.31	172	250	15.3	0	0.0	156	4.3	203	5.4	219	7.7	207	8.2	0.8		
79.98	125	165	4.4	187	3.7	0	0.0	162	3.2	167	3.3	170	3.7	0.4		
84.5	-4	202	9.8	199	7.7	222	5.0	0	0.0	188	7.9	203	7.6	0.8		
85.44	-37	0	0.0	155	4.4	0	0.0	0	0.0	240	8.6	197	6.5	0.7		
87.89	-128	236	11.2	212	9.6	270	12.9	244	12.1	0	0.0	241	11.4	1.1		
89.28	-173	0	0.0	0	0.0	0	0.0	190	5.6	164	3.7	177	4.7	0.5		
90.53	**-214**	276	18.8	286	26.1	278	16.5	296	18.1	241	6.9	275	17.3	1.7		
91.72	-251	0	0.0	0	0.0	0	0.0	227	10.4	244	12.5	236	11.4	1.1		
94.83	-347	0	0.0	191	4.6	198	5.9	216	8.7	0	0.0	201	6.4	0.6		
97.16	**-426**	331	22.6	228	15.4	403	35.2	436	48.5	675	75.0	414	39.3	3.9		
97.31	-431	0	0.0	131	2.9	0	0.0	0	0.0	0	0.0	65	1.5	0.1		
100.19	**-529**	219	12.1	224	6.6	0	0.0	247	15.9	235	7.7	231	10.6	1.1		

Table 3 – Statistics on sulfate signal for identical peaks in core 1, 2, 3, 4 and 5. Geometric standard deviations are calculated on peaks heights (i.e maximum concentration reached, in $ng.g^{-1}$) and on peaks sulfate flux (i.e total mass of volcanic sulfate deposited after the eruption). Background corrections are based on background values calculated separately for each volcanic event.

Study	Number of compared cores	Geom. std deviation based on maximum concentration	Geom std deviation based on deposition flux
Wolff and others	2	1.5	
This study	2*	1.35	1.56
This study	5	1.21	1.41

* : C_x/C_1 , with x=2,3,4,5

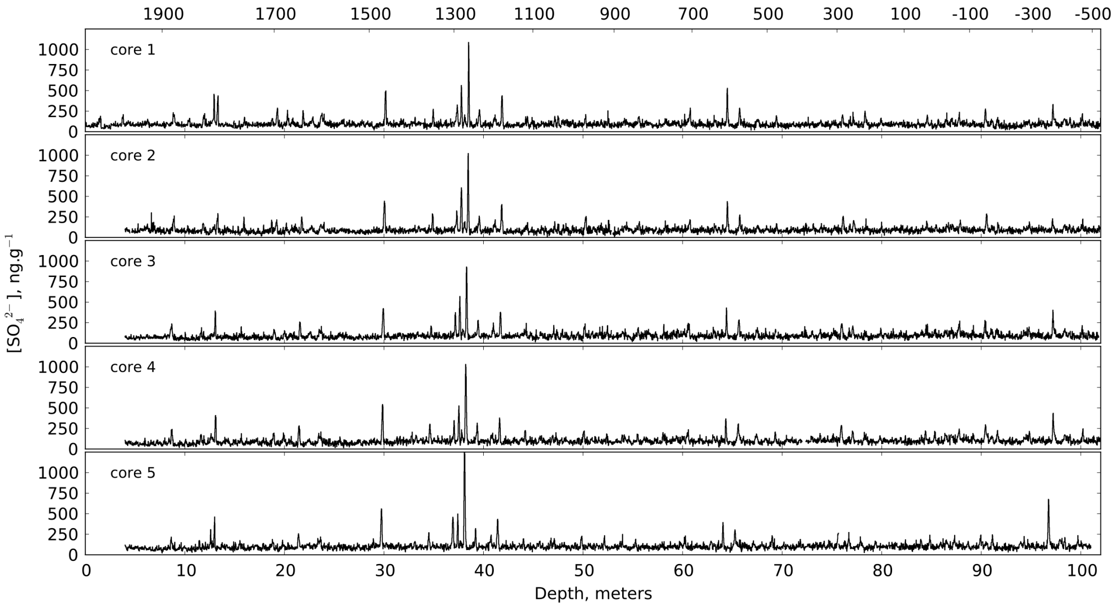

Figure 1 - Sulfate profiles on the 5 replicate cores obtained during a drilling operation at Dome C – Antarctica in 2011.

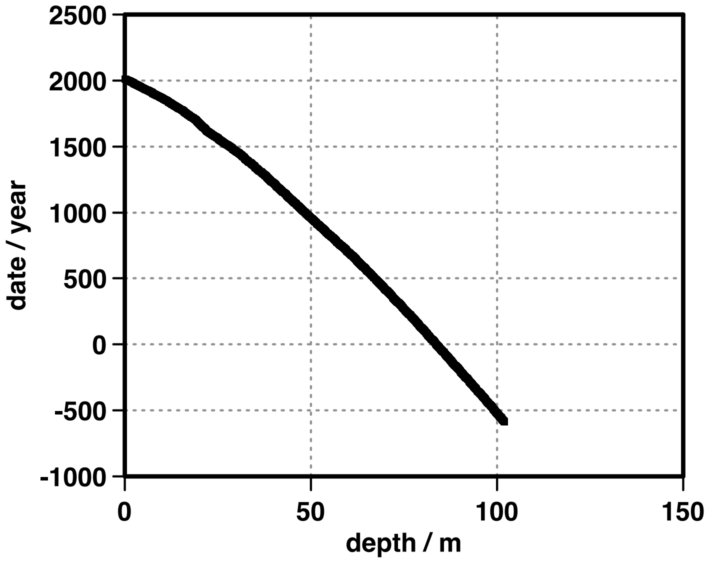

Figure 2 - Age versus depth in core 1 drilled in 2011 CE, Dome C – Antarctica

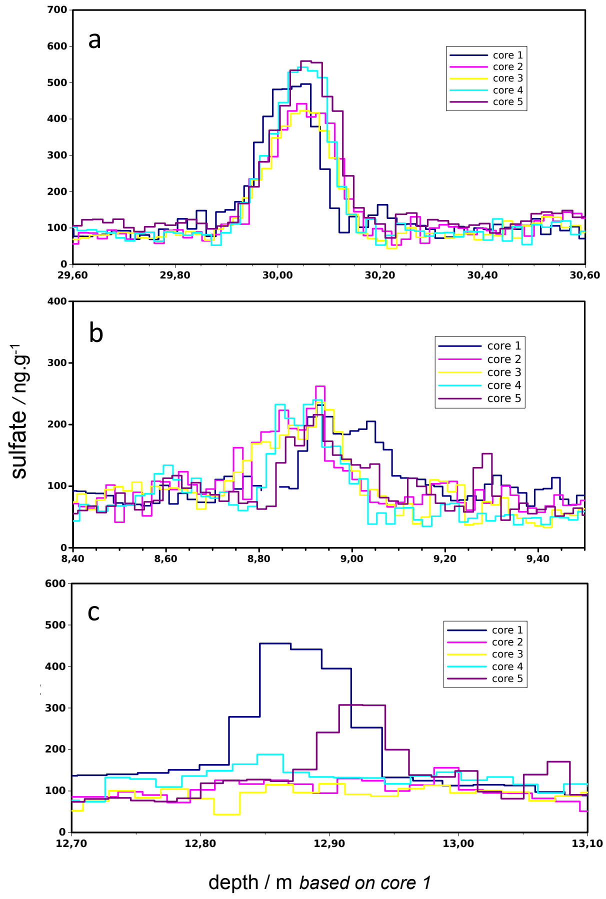

Figure 3 –Kuwae (a, top), Krakatoa (b, middle) and Tambora (c, bottom) sulfate concentration profiles after depth synchronization. All peaks are within a 20 cm uncertainty, enabling to clearly attribute each occurrence to a single event.

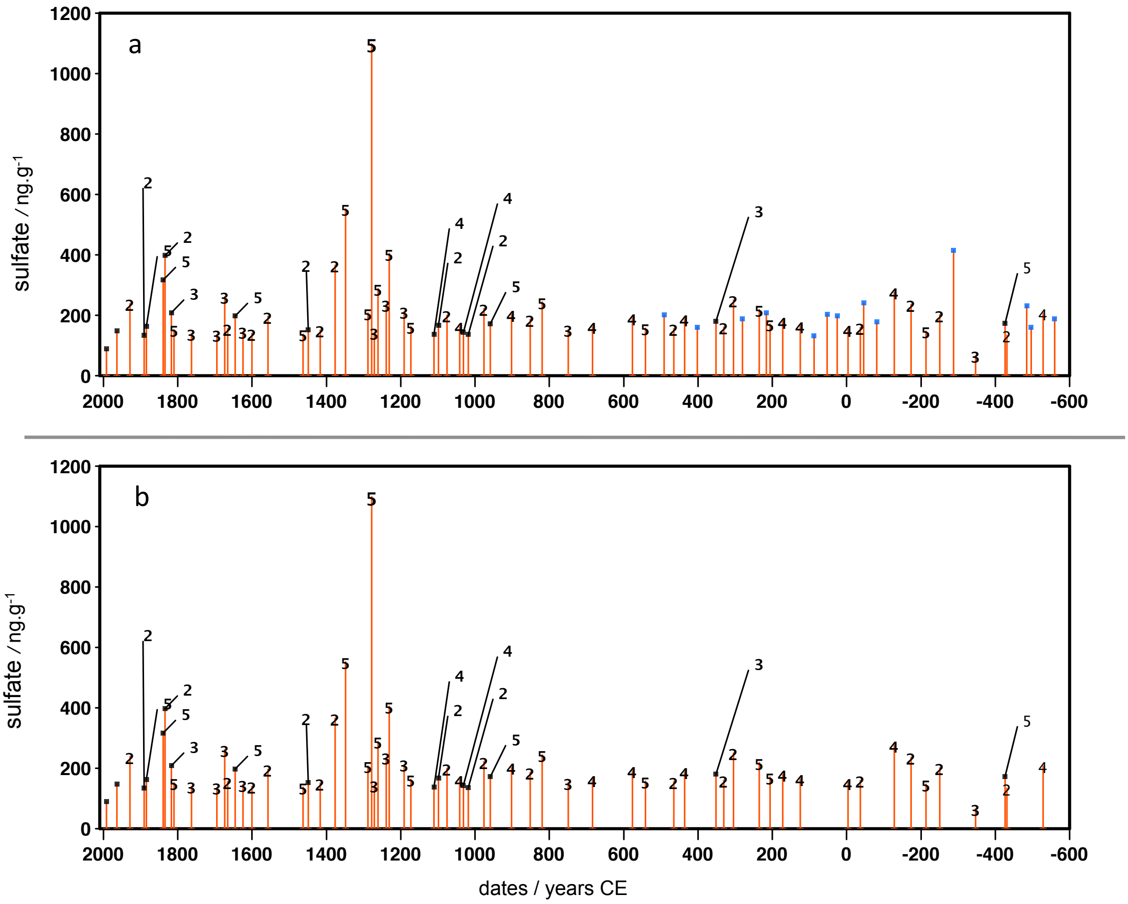

Figure 4 – a) Composite sulfate peak profile deduced from our statistical analysis of the 5 cores using our detection peak and synchronization algorithms (see text). The numbers indicate the number of time a common peak is found in the cores. Unnumbered peaks, peaks found only in single core. b) same as a) without the single detected peaks. All the remaining peaks are considered as volcanic eruptions. See Table 2 for details.

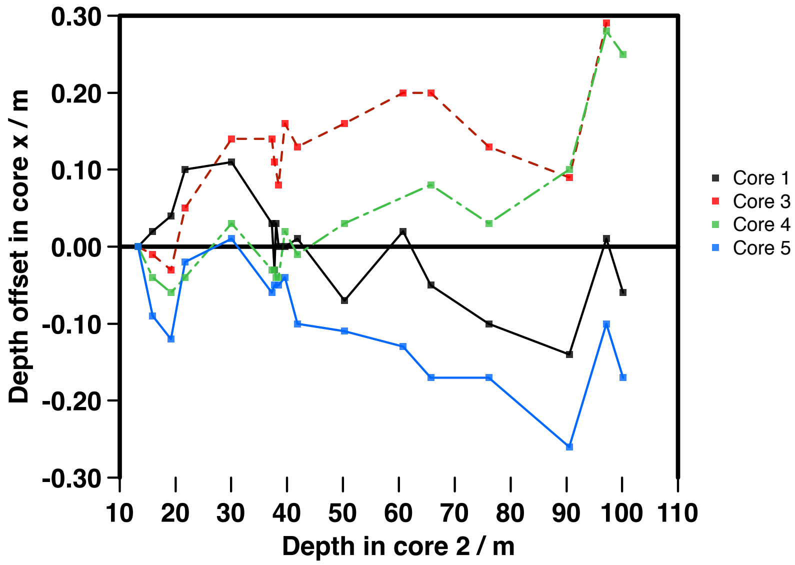

Figure 5 – Depth offset of 18 common and well-identified volcanic events in cores 1, 3, 4 and 5 relatively to core 2. To overcome offset due to the drilling process and poor core quality on the first meters, UE 1809 (depth ca. 13 m) is taken as the origin and horizon reference.

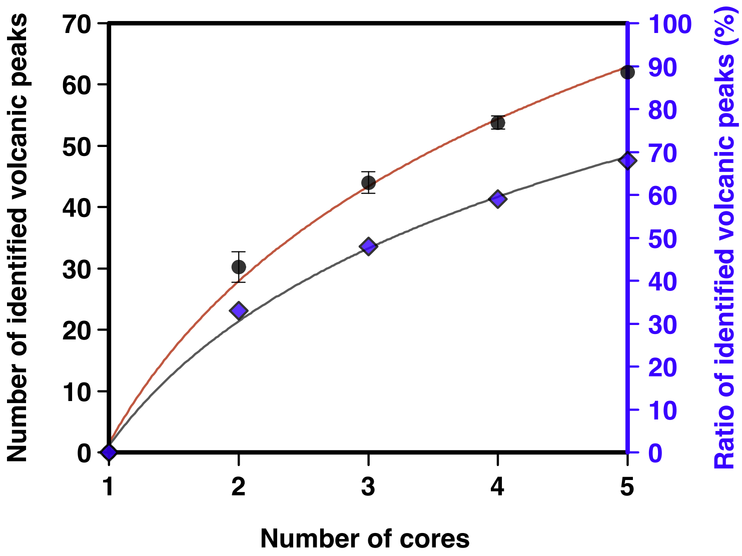

Figure 6 – Black dots with red line (left axis) represent the number of sulfate peaks that can be identified as volcanic peaks in a composite profile, made of n cores (with n ranging from 1 to 5). A sulfate peak appearing simultaneously in at least two cores is considered to be a volcanic peak. Blue diamonds represent the ratio of identified volcanic peaks, i.e the number of identified volcanic peaks (plotted on the left axis), relatively to the total number of sulfate peaks (no discrimination criteria) in a composite made of 5 cores. In our case, the 5 ice-cores composite comprises 91 sulfate peaks (Agung and Pinatubo excluded). With two cores, only 33% of them would be identified as being volcanic peaks (detected in both cores), while 68% of them can be identified as volcanic events using 5 cores.

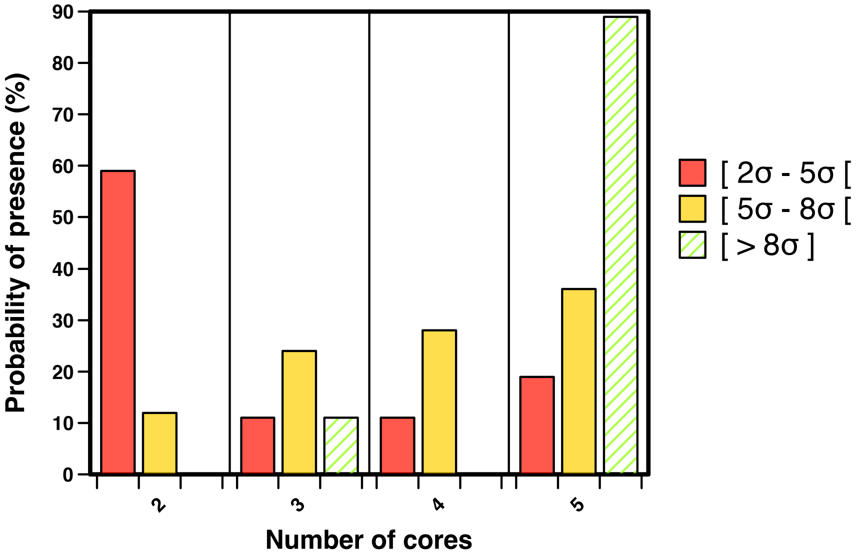

Figure 7 - Peaks probability to be detected in 2, 3, 4 or 5 cores, as function of their flux. The three categories of flux are defined by peaks flux value, relatively to the average flux, and quantified by x time (2, 5 and 8) the flux standard deviation, calculated for a 30 ppb standard deviation in concentrations.

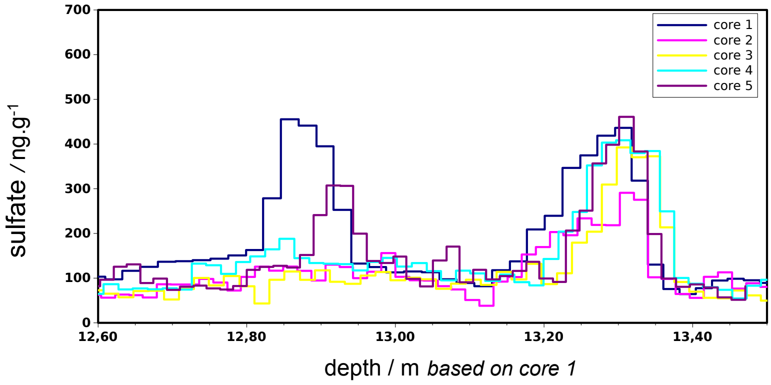

Figure 8: Close look at UE 1809 and Tambora (1815) events showing the absence of the Tambora event in 2 out of the 5 cores. This figure illustrates the possibility of missing major volcanic eruptions when a single core is used.

SOM

1. Gfeller *et al*. (2014) approach on Dome C 5 cores: calculation of the representativeness

n *(number of cores)*	1	2	3	4	5
$\tilde{R}^2_{n,\infty}$ SO_4^{2-}	**0.72**	**0.84**	**0.89**	**0.91**	**0.93**

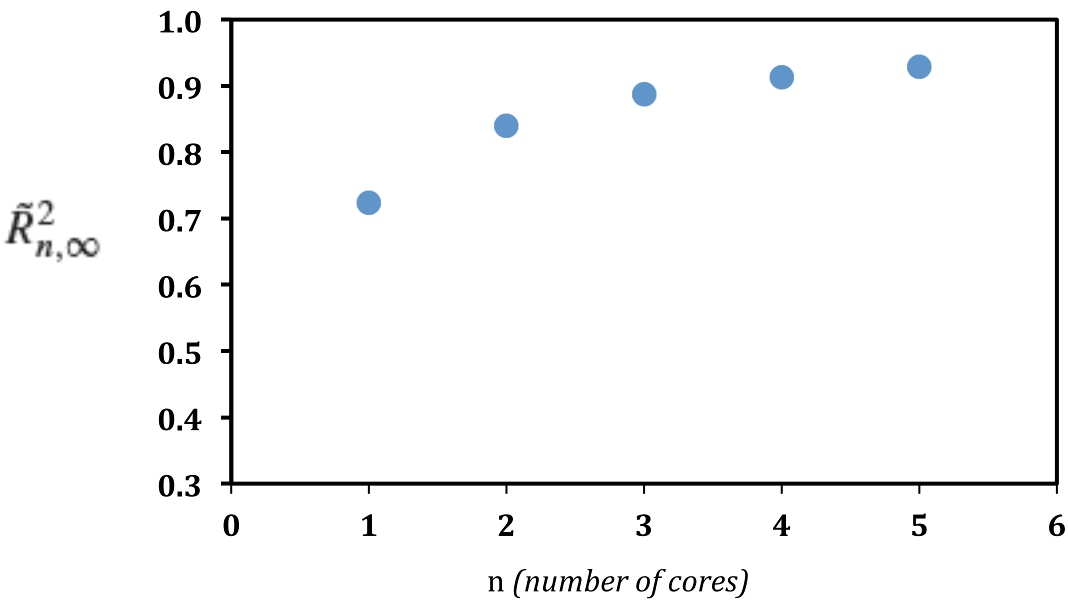

Figure S1: Representativeness of sulfate in the cores depending on the number of cores n (based on Gfeller et al., 2014 approach).

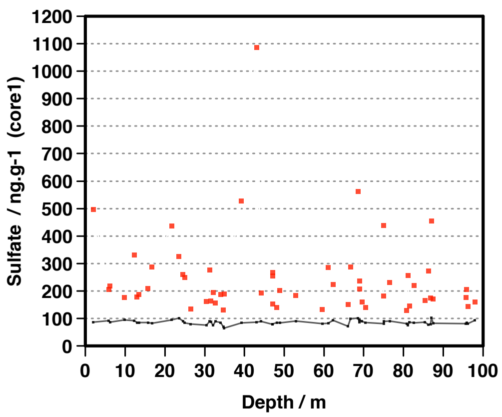

Figure S2 - Variation of the background along depth in core 1, red dots are detected peaks, the dark line stands for the background concentration.